NASA Technical Memorandum 103651

Thermal and Structural Assessments of a Ceramic Wafer Seal in Hypersonic Engines

Mike T. Tong
Sverdrup Technology, Inc.
Lewis Research Center Group
Brook Park, Ohio

and

Bruce M. Steinetz
National Aeronautics and Space Administration
Lewis Research Center
Cleveland, Ohio

NASA

THERMAL AND STRUCTURAL ASSESSMENTS OF A CERAMIC WAFER

SEAL IN HYPERSONIC ENGINES

Mike Tong
Sverdrup Technology, Inc.
Lewis Research Center Group
Brook Park, Ohio 44142

and

Bruce Steinetz
National Aeronautics and Space Administration
Lewis Research Center
Cleveland, Ohio 44135

Abstract

This paper numerically assesses the thermal
and structural performances of a ceramic wafer seal
in a simulated hypersonic engine environment. The
effects of aerodynamic heating, surface contact
conductance between the seal and its adjacent sur-
faces, flow of purge coolant gases, and leakage of
hot engine flow path gases on the seal temperature
were investigated from the engine inlet back to the
entrance region of the combustion chamber. Finite
element structural analyses, coupled with Weibull
failure analyses, were performed to determine the
structural reliability of the wafer seal.

Introduction

Key to the development of a single-stage
Earth-to-Orbit vehicle is an advanced propulsion
system integrally designed with the airframe. To
maintain sufficiently high specific impulse and
reach orbital velocity (Mach 25), a hydrogen-
burning, hypersonic engine is being developed by
NASA. A critical mechanical system in this
advanced hypersonic engine is the panel-edge seal
system that seals gaps between the articulating
engine panels and the stationary side walls (split-
ter walls). These seals must prevent the extremely
hot, pressurized engine flow-path gases and poten-
tially explosive hydrogen-oxygen mixtures from
leaking past the movable panels and damaging the
engine panel support and articulation systems.

Four panel-edge seal concepts were investi-
gated by NASA Lewis Research Center (Ref. 1). The
results showed that the ceramic wafer seal concept
had the best sealing performance. Room temperature
leakage measurements showed that it had the lowest
leakage rate among the four seal concepts. Its
leakage was less than the tentative leakage limit
of 0.006 kg/s-m of seal (0.004 lbm/s-ft of seal),
for all the measured combinations of seal preload,
pressure differential, and wall distortion. The
tentative leakage limit was established based on
the balanced-pressure approach as explained in
Ref. 1. Because of its superior performance, the
ceramic wafer seal was chosen for the present
study.

The ceramic wafer seal is made of stacked
ceramic wafers mounted in a seal channel along the
edge of the movable engine panel, as shown in
Fig. 1. The seal conforms to the engine wall dis-
tortions by relative sliding of adjacent wafers.
Various techniques can be used to preload the
ceramic wafers against the engine wall, such as a
cooled pressurized metal bellow that presses
against the backside of the seal.

The objective of this paper is to assess the
thermal and structural performances and the statis-
tical reliability of the ceramic wafer seal concept
under simulated hypersonic engine heating condi-
tions. It builds upon the thermal and structural
analyses conducted in Refs. 2 and 3. Boundary
layer and thermal analyses were performed to deter-
mine if the seal temperature exceeded the 1371 °C
(2500 °F) allowable operating temperature for a
silicon carbide wafer seal. Finite element struc-
tural analyses, coupled with Weibull failure analy-
ses, were performed to determine the structural
reliability of the wafer seal.

Numerical Models

PATRAN II, a finite-element pre- and post-
processor, is used to create the finite element
models. The thermal analysis model had 640 four-
node elements and 779 nodes. The seal was modeled
as being in contact with both upper and lower inner
surfaces of the panel and the splitter wall, as
shown in Fig. 2. To facilitate the reliability
analysis, a three-dimensional model was used for
the stress analysis. The stress analysis model had
1632 eight-node brick elements and 2704 nodes. Gap
elements were used to model the contacts between
the seal and the panel/splitter wall. This would
allow the wafers to locally expand, move along the
adjacent surfaces, and even move away from the sur-
face to accommodate thermal distortions. The model
is shown in Fig. 3. Translation software was used
to convert the PATRAN models to data useful to
MARC, a general purpose finite element program.

Analytical Procedures

Problem Description

The seal analyzed in this study was made of
silicon carbide, because of its relatively high
thermal conductivity compared with other ceram-
ics. It measured 13 by 13 by 3 mm (0.5 by 0.5 by
0.125 in.). The seal was recessed 3 mm (0.125 in.)
below the panel surface and the exposed seal width
was also 3 mm (0.125 in.). The size and the loca-
tion of the seal is similar to the one being tested
at NASA Lewis (Ref. 4). Heat dissipation of the
seal was by means of conduction to the top and bot-
tom panel surfaces, and the splitter wall (provided
the seal is in contact with the wall).

Two engine locations were selected for detailed thermal and structural analyses of wafer seals, both were on the engine cowl. The first region analyzed was on the engine inlet ramp where pressures and temperatures are relatively modest. The second region was the combustor entrance region where heat flux rates were most severe, as indicated below. The two locations are shown in Fig. 4.

Steady State Thermal Analysis

Analysis of panel-edge seals requires understanding the flow fields in the engine. The engine flow field determines the environment to which the seal would be subjected. The aero-thermal boundary conditions used for the analyses were generated using several computer codes. RAMSCRAM (Ref. 5), a one-dimensional ramjet/scramjet engine simulation code which takes into account the real gas effects (thermodynamics equilibrium), was used to calculate the engine flow free stream velocities, temperatures, and pressures as a function of freestream Mach number, engine station and trajectory. These freestream velocities, temperatures, and pressures were used by the boundary layer code, STAN5 (Ref. 6), to calculate the heat flux rates into the exposed top surface of the seal. For assessment purposes, all the analyses were conducted using the most severe heat flux conditions, i.e., the effect of the seal recess depth on the heat flux was neglected.

The results from the aerothermal analyses showed that one of the most severe aerothermal environments for the seals occurred at Mach 10, where pressure differential reached 0.59 MPa (85 psi), engine static temperature reached 2704 °C (4900 °F), and combustor entrance heat flux rates were as high as 13165 kw/m^2 (1160 Btu/ft^2-sec). The result is shown in Fig. 5. For this reason, the Mach 10 flow condition was chosen for all the analyses.

Both the splitter wall and engine panel were assumed to be actively cooled to 649 °C (1200 °F). Two contact conductances were considered: 1420 and 8512 W/m^2-K (250 and 1500 Btu/ft^2-hr-R). These conductances represent a range of conductances typical of ceramic to metal contacts (Ref. 7). The surface contact conductance is strongly dependent on the conditions of the mating surfaces and contact pressure. The thermal boundary conditions are shown schematically in Fig. 6.

Once the boundary conditions were determined, the MARC finite element program (Ref. 8) was used to determine the temperature distribution within the seal.

In the cases where the gap was open between the seal and the splitter wall, a one-dimensional compressible flow energy equation (Ref. 9):

$$dM^2 = F_t \frac{dT_o}{T_o} + F_f 4f \frac{dx}{2D}$$

where

$$F_t = \frac{M^2(1 + kM^2)\left(1 + \frac{k-1}{2} M^2\right)}{1 - M^2}$$

$$F_f = \frac{kM^4\left(1 + \frac{k-1}{2} M^2\right)}{1 - M^2}$$

T_o stagnation temperature

M   Mach number

f   friction coefficient

D   gap spacing

k   ratio of specific heats

x   leakage distance

was solved numerically to determine the convective boundary condition for the seal nose. The equation calculates the velocities, temperatures, and pressures of leakage gas (or purge coolant) as a function of leakage distance. Since leakage gas temperature and seal nose temperature are interdependent, the equation was solved iteratively with MARC. The solution converged and resulted in final seal temperatures when the seal boundary and leakage gas were in thermal equilibrium. In addition to the convective boundary conditions, thermal radiation was assumed between the seal nose and the splitter wall. However, it was found later that the effect of the thermal radiation has insignificant effect on the seal temperature.

For the case with purged helium flow, it was assumed that the small gap between the seal nose and the splitter wall was purged with 21 °C (70 °F), 0.10 MPa (15 psi) helium from below the wafer seal. The resulting force urged the seal up and in contact with the top panel. There was no contact between the lower surface of the seal and the engine panel (Fig. 7).

Structural Analysis

A structural analysis was conducted on the ceramic wafer seal operating in the combustor entrance region where the heat flux rates are severe. The boundary conditions for the structural analyses are shown schematically in Fig. 7. The analysis was conducted using the MARC finite element program. Seal temperatures calculated by thermal analysis (with purged helium cooling) were used for the analyses, with the assumption of no thermal gradient through the 3 mm (0.125 in.) thickness of the seal. In addition to the thermal boundary conditions, the following mechanical boundary conditions were also used: 0.55 to 0.83 MPa (80 to 120 psi) preloads along the backside of the ceramic wafers; 0.10 MPa (15 psi) purge helium pressure along the bottom surface of the seal.

Reliability Analysis

Due to the brittle nature of ceramics and the statistical nature of their flaw populations, reliability analysis is essential for determining the survivability of the ceramic wafer seal. In the current study, the probabilistic design methodology of combining the Weibull statistics of silicon carbide (two parameter) with linear fracture mechanics theory was used to determine the fast fracture reliability of the wafer seals. This methodology is utilized by the computer program, CARES (Ceramic Analysis and Reliability Evaluation of Structures, Ref. 10), developed by NASA Lewis. The probabilistic approach provides a realistic way to assess the structural performance of wafer seals, because it accounts for the effect of flaw population in the ceramics used for the seal fabrication.

In performing the Weibull failure analysis, the Weibull distribution for the silicon carbide was integrated with the stress and temperature distributions for the wafer seal. Both temperature and stress distributions were obtained by finite element analyses. Weibull distribution for the Carborundum silicon carbide material were provided by the University of Dayton Research Institute (Ref. 11). Their test data indicated a majority of the failures of the test specimens were due to the surface flaws (over 93 percent). For this reason, only surface flaw analyses were conducted in the current study. Shetty's semiempirical fracture criterion (Ref. 12), with a shear sensitivity factor of 0.80, was used in all the current analyses. The material surface flaws were modeled as semicircular cracks.

Results and Discussion

Using the analytical and the boundary conditions just described, a parametric study was conducted to evaluate maximum seal temperatures over a range of simulated engine inlet and combustor entrance heat flux rates obtained from the flow analyses.

Thermal Analysis of Wafer Seal in the Engine Inlet Region

The results shown in Fig. 8 show that even with very poor contact conductance, the maximum seal temperature was less than 1149 °C (2100 °F), below the 1371 °C (2500 °F) allowable operating temperature for silicon carbide ceramic wafers. Based on these results, active cooling of the wafer seals in the engine inlet will not be required at Mach 10 flight conditions. Seal temperature distribution for an upper range engine inlet heat flux rate of 3405 kW/m^2 (300 Btu/ft^2-sec) is shown in Fig. 9.

A study was conducted to evaluate the effects of flow path gas leakage on the maximum seal temperature over the same range of engine inlet heat fluxes. A 0.018 mm (0.0007 in.) gap was introduced between the nose of the seal and the splitter wall through which a small amount of 0.03 MPa (5 psi) inlet air at 316 °C (600 °F) leaked. This leakage gas temperature is based on the flow analysis of a generic hypersonic engine flying a 0.07 MPa (1500 lb/ft^2) flight trajectory. Only a slight increase in temperature (6 °C or 10 °F) was observed over the full heat flux ranges. The slight increase in temperature was mainly due to the loss of contact conductance between the seal nose and the splitter wall. The results are shown in Fig. 10.

Thermal Analysis of Wafer Seal in the Combustor Entrance Region

The results shown in Fig. 11 indicate that the maximum seal temperature is very sensitive to the contact conductance. For good contact conductance (8512 W/m^2-K or 1500 Btu/ft^2-hr-°R), the maximum seal temperatures were slightly above the allowable operating temperature of 1371 °C (2500 °F). However, for poor contact conductance (1420 W/m^2-K or 250 Btu/ft^2-hr-°R), the maximum seal temperature far exceeded the allowable operating temperature over the full heat flux range. This clearly indicates that some form of active cooling is required for the wafer seals operating in the combustor

environment. For the current study, purged helium cooling was chosen. For this study there was no coolant on the backside of the seal.

In general, for a given seal contact condition, the maximum seal temperature can be related to the thermal resistances due to seal thermal conductivity and surface contact conductance, as follows:

$$T_{max} - T_w = Q\left(\frac{w}{w_s}\right)^n\left(K_1\frac{1}{CA_c} + K_2\frac{w}{kA_c} + K_3\frac{w_s}{kA_c}\right)$$

where

T_{max}	maximum seal temperature
T_w	wall temperature
Q	heat flux on the seal
w	seal recess gap width
w_s	seal size, width
K_1, K_2, K_3, n	constants
C	contact conductance per unit area
k	seal thermal conductivity at maximum seal temperature
A_c	total seal contact area with panels and splitter wall

The first two terms on the right hand side of the equation accounts for the thermal load on the seal. The second term of the equation accounts for the external thermal resistance due to the surface contact conductance between the seal and its adjacent surfaces. Internal thermal resistances due to recess gap width and seal size are accounted by the last two terms of the equation. The four parametric constants can be determined from four baseline finite element or finite difference analyses. Figure 12 shows that the above relation correlates well with the finite element results. The equation can be used to aid the design of wafer seals.

The effect of purged helium cooling on the maximum seal temperatures is shown in Fig. 13. Maximum seal temperatures were lowered by 167 to 222 °C (300 to 400 °F) for the high contact conductance, and by 1111 to 1444 °C (2000 to 2600 °F) for the lower contact conductance. The helium's high thermal capacity and the high heat transfer film coefficient in the seal gap (due to low Reynolds number, friction dominated flow) drastically reduced the maximum seal temperatures to below the 1371 °C (2500 °F) operating limit. The helium mass flow rate was 3×10-5 kg/m-sec (2×10-5 lbm/ft-sec) for both contact conductance conditions. Besides cooling the seal, the purged helium also helps to prevent hot and potentially explosive hydrogen-oxygen mixtures from escaping through the seal systems and damaging engine panel support and articulating systems. The seal temperature distribution is shown in Fig. 14.

The helium flow rates were calculated by numerically solving the one-dimensional compressible flow equation described above, with a gap of 0.018 mm (0.0007 in.). To determine the sensitivity of purge helium flow rate to gap size, the helium mass flow rate was recalculated for a 0.038 mm (0.0015 in.) gap. By doubling the gap

size the purge flow rate increased by about ten-fold. This indicates the need to maintain small gaps to conserve the coolant resources.

Effect of Seal Recess Gap Depth

For assessment purposes, all the thermal analyses performed were based on the most severe thermal conditions, i.e., zero seal recess gap depth. By recessing the seal away from the engine chamber, the thermal load on the seal should be reduced. A one-dimensional gap flow analysis shows that the thermal load on a recessed seal can be approximated as follows:

$$\frac{Q}{Q_o} \simeq 1 - \frac{\left(1 - e^{\frac{-fh}{w}}\right)(T_g - T_w)}{(T_g - T_s)}$$

where

Q_o heat flux on a seal at $h/w = 0$

Q heat flux on a recessed seal at a given h/w

w seal recess gap width

h seal recess gap depth

f friction coefficient $= 12 \ \mu/\dot{m}$

$\dot{m}$ gap mass flow rate per unit length of seal

μ dynamic viscosity of hot gas

T_g stagnation gas temperature at $h/w = 0$

T_s given maximum allowable seal temperature

T_w wall temperature

For the case that $T_g \gg T_s$ and T_w as in the combustor entrance region, or when the seal and its adjacent panels are maintained at the same temperature by the coolant, i.e., $T_s = T_w$,

$$\frac{Q}{Q_o} \simeq \exp\left(\frac{-fh}{w}\right)$$

The effect of h/w ratio on the thermal load to the seal in the combustor entrance region is shown in Fig. 15 for $T_s = T_w$. The result was generated based on the gap flow rate of 0.006 kg/s-m (0.004 lbm/s-ft of seal, tentative leakage limit). It shows that by recessing the wafer seal away from the engine panel surface, the thermal load on the seal can be reduced significantly. This is important since it implies the possibility of the wafer seal to survive the heat fluxes in the combustor entrance region with minimal active cooling. Thus the h/w ratio is an important parameter in designing the panel-edge seal system.

While this analysis does not compute the three-dimensional flow field, it suggests that the actual thermal load on a recessed wafer seal is considerably less than the thermal load in the engine chamber. Preliminary three-dimensional flow field analyses of the seal gap (Refs. 13 and 14) also indicated much reduced thermal load on the seal caused by the rapid expelling of the flow from the seal gap recess. In comparison to the results from the preliminary three-dimensional flow field analysis, the prediction by the current one-dimensional flow analysis is more conservative.

Structural and Reliability Analyses of Ceramic Wafer Seal in the Combustor Entrance Region

Maximum principal stress distribution of the ceramic wafer seal is shown in Fig. 16. The maximum tensile stress of 162 MPa (23.5 ksi) located at the nose of the seal is below the tensile strength of the material (241 MPa or 35 ksi). The minimum principal stress, -203 MPa (-29.5 ksi), was a small percentage of the silicon carbide's 3862 MPa (560 ksi) compressive strength. Increasing the preload on the backside of the seal from 0.55 to 0.83 MPa (80 to 120 psi) essentially did not change the stress level. It indicates the seal stresses were primarily induced by the thermal gradients. The results are shown in Table I.

Weibull failure analyses show that the probability for the wafer seal to survive is very high, over 99.99 percent. This is because of the low stress level of the seal and the excellent material strength of the silicon carbide used for the seal fabrication. Weibull material data indicates the silicon carbide has a scale parameter of 281 MPa (40.5 ksi, corresponds to the stress level where 63.2 percent of specimens with unit volumes would fracture) and a shape parameter (or Weibull modulus) of 10.45 at 1200 °C (2192 °F). The shape parameter describes the degree of strength variability of a ceramic material. Since the scale parameter and the shape parameter are processing dependent, good quality control during the seal fabrication process is essential to ensure survivability of the wafer seal in the hypersonic engines.

Based on the results from the Weibull analyses of the wafer seal in the combustor entrance region, it can be concluded that the probability of survival for the wafer seals in the engine inlet region should be even higher. The heat flux rates in the engine inlet are much less severe than in the combustor entrance region.

Summary and Conclusion

Based on the results from the steady state analyses, the following summaries and conclusions are made for the silicon carbide wafer seal in a hypersonic engine:

1. Coolant is not required for the wafer seals in the engine inlet region for the Mach 10 flow condition. The wafers seals have an excellent chance to survive in this region.

2. The leakage of incoming flow path gas has insignificant effect on the seal temperature in the engine inlet region.

3. With shallow seal recess gap depth considered (3 mm or 0.125 in.), active cooling will be required for the wafer seals in the combustor entrance region, because of the high heat fluxes in this region.

4. Active cooling of the wafer seals in the combustor entrance region with purged helium gas is effective in reducing the seal temperature to below the operating temperature limit of silicon carbide material. Furthermore, the purged helium helps to prevent hot and potentially explosive hydrogen-oxygen mixtures from escaping through the seal

systems and damaging engine panel support and articulation systems.

5. The heat fluxes on the seal can be reduced significantly (thus reducing the seal temperature) by locating the wafer seal away from the engine chamber, i.e., by increasing the seal recess gap depth.

6. Active cooling of the seal, combined with good quality control in fabrication of the silicon carbide wafer seals, will ensure survivability of the wafer seal in the combustor entrance region.

7. The probabilistic design methodology of combining the Weibull statistics of silicon carbide with the linear fracture mechanics theory was used to determine the structural reliability of the wafer seal. This methodology provides a realistic way to assess the structural performance of ceramic wafer seals, because it accounts for the flaw population in the ceramics used for the seal fabrication.

Acknowledgment

The authors gratefully acknowledge Leo Burkardt of the NASA Lewis Research Center for performing the hypersonic engine cycle analysis.

References

1. Steinetz, B.M., DellaCorte, C., and Sirocky, P.J., "On The Development of Hypersonic Engine Seals," NASA TP-2854, 1988.

2. Steinetz, B.M., Tong, M., and Coirier, W.J., "Seal Thermal Analysis of Panel-Edge Seals for Hypersonic Engines," NASA CP-6039, Vol. VI, Structures, May, 1989.

3. Steinetz, B.M., DellaCorte, C., and Tong, M., "Seal Concept and Material Performance Evaluation for the NASP Engine," NASA CP-7045, Vol. VI, Structures, Nov. 1989.

4. Steinetz, B.M., "A Test Fixture for Measuring High-Temperature Hypersonic Engine Seal Performance," NASA TM-103658, Dec. 1990.

5. Burkardt, L.A. and Franciscus, L.C., "RAMSCRAM - A Flexible Ramjet/Scramjet Engine Simulation Program," NASA TM-102451, 1990.

6. Crawford, M.E. and Kays, W.M., "STAN5 - A Program for Numerical Computation of Two-Dimensional Internal and External Boundary Layer Flows," NASA CR-2742, 1976.

7. Dursch, H.W., Nedervelt, P.D., Newquist, C.W., and Burns, R.A., "National Aerospace Plane (NASP) Airframe Technology Option Five, Sealing Concepts," Boeing Report, D180-31720-1.

8. MARC General Finite Element Program, MARC Analysis Research Corporation, Palo Alto, CA.

9. Shapiro, A.H., The Dynamics and Thermodynamics of Compressible Fluid Flow," The Ronald Press Company, New York, 1953..

10. Nemeth, N.N., Mandersheid, J.M., and Gyekenyesi, J.P., "Ceramics Analysis and Reliability Evaluation of Structures (CARES)," NASA TP-2916, 1989.

11. Hecht, N.L., "Environmental Effects in Toughened Ceramics," Ceramic Technology for Advanced Heat Engines Project, Bi-Monthly Report to DOE Office of Transportation Systems, June-July 1989, ORNL/CF-89/252, Oak Ridge National Laboratory, 1989.

12. Shetty, D.K., "Mixed Mode Fracture Criteria for Reliability Analysis and Design With Structural Ceramics," Journal of Engineering for Gas Turbines and Power, Vol. 109, No. 3, July 1987, pp. 282-289.

13. Coirier, W.J., "High Speed Corner and Gap-Seal Computations Using an LU-SGS Scheme," AIAA Paper 89-2669, July 1989 (also, NASA TM-102138).

14. Coirier, W.J., "Efficient Real Gas Navier-Stokes Computations of High Speed Flows Using An LU Scheme," AIAA Paper 90-0391, Jan. 1990 (also, NASA TM-102429).

TABLE I. - SUMMARY OF STRESS ANALYSIS RESULTS FOR THE WAFER SEAL IN THE COMBUSTOR ENTRANCE REGION WITH HELIUM COOLING

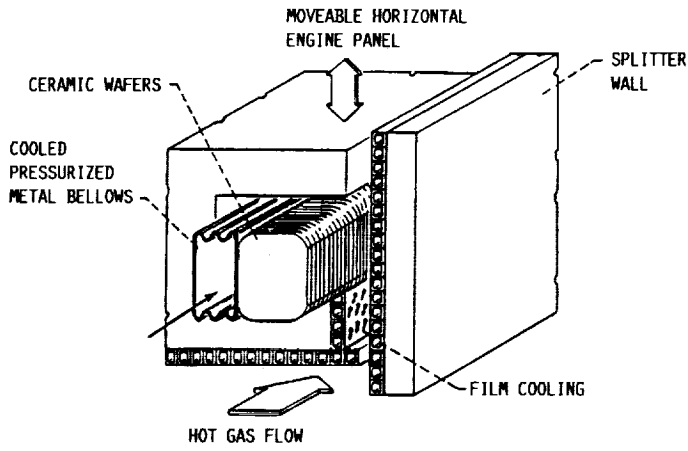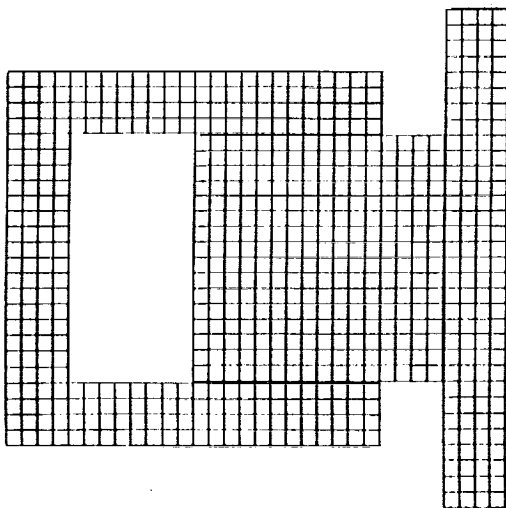| Seal preload,		Maximum principal stress,		Minimum principal stress,		Probability of survival, percent
MPa	ksi	MPa	ksi	MPa	ksi	
0.55	0.08	162	23.5	-203	-29.5	99.996
.83	.12	162	23.5	-203	-29.5	99.996

FIGURE 1. - CERAMIC WAFER SEAL CONCEPT.

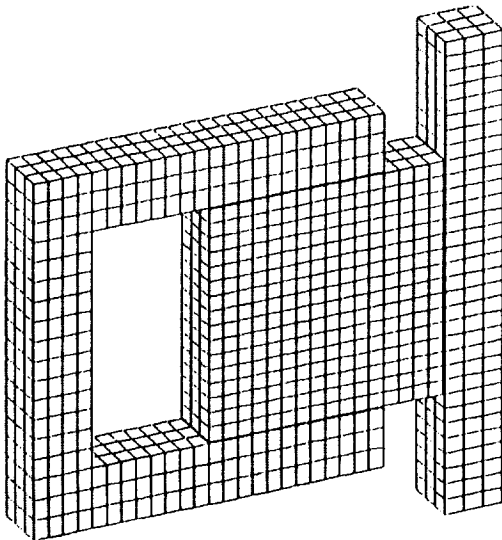FIGURE 2. - FINITE ELEMENT MODEL FOR THERMAL ANALYSES.

FIGURE 3. - FINITE ELEMENT MODEL FOR STRESS ANALYSES.
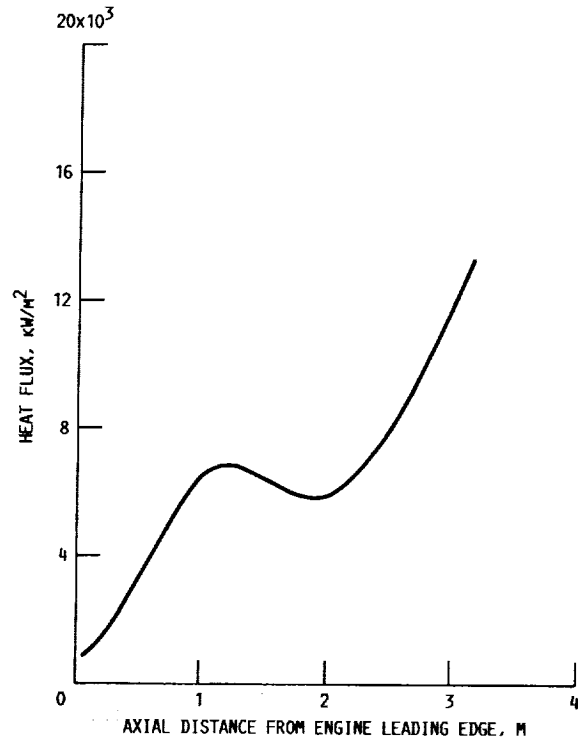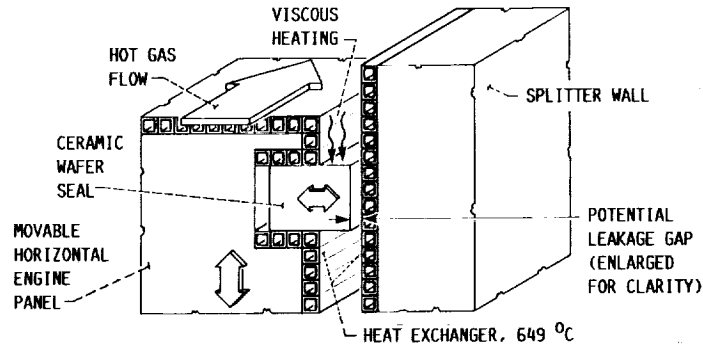

FIGURE 4. - ENGINE LOCATIONS FOR SEAL THERMAL ANALYSIS.

FIGURE 5. - HEAT FLUX DISTRIBUTION IN THE ENGINE INLET
AND COMBUSTOR ENTRANCE REGION.

6

GAP CONDITIONS:	THERMAL BOUNDARY CONDITIONS:
• CLOSED	• CONDUCTION: CONTACT CONDUCTANCE (1420 OR 8512 W/M^2-K)
• PURGED WITH WITH HELIUM GAS	• GAS COOLS SEAL • THERMAL RADIATION BETWEEN SEAL NOSE AND SIDEWALL
• SMALL LEAKAGE OF FLOWPATH GAS	• LEAKAGE GAS HEATS SEAL • THERMAL RADIATION BETWEEN SEAL NOSE AND SIDEWALL

FIGURE 6. – THERMAL ANALYSIS BOUNDARY CONDITIONS.

$(M_\infty = 10)$
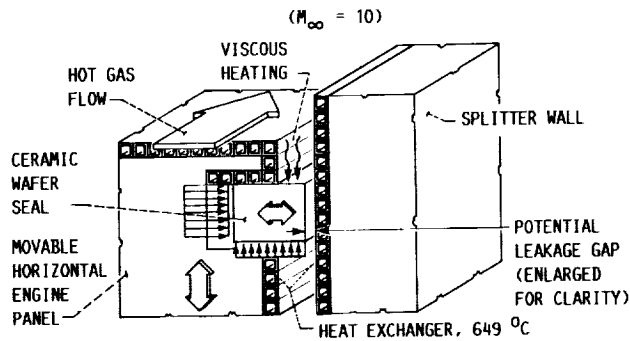
THERMAL

VISCOUS HEATING = 13165 KW/M^2

GAP PURGED WITH 21 ^{O}C He GAS

TOP OF SEAL IN CONTACT WITH SEAL CHANNEL:

CONTACT CONDUCTANCE = 1420 W/M^2-K

STRUCTURAL

BELLOW PRELOAD = 0.55 MPa

He PURGE PRESSURE = 0.10 MPa

FIGURE 7. – STRUCTURAL ANALYSIS BOUNDARY CONDITIONS.
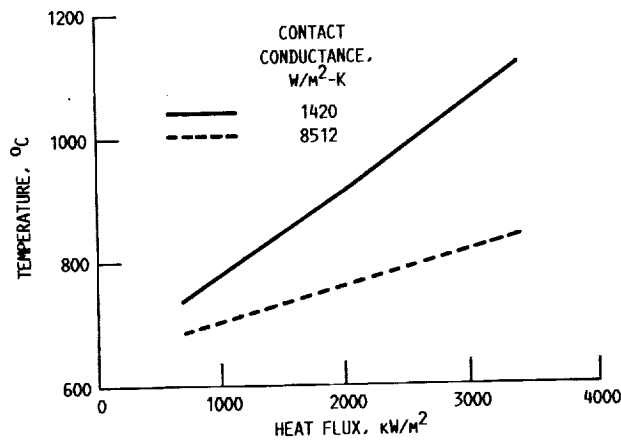
FIGURE 8. – MAXIMUM SEAL TEMPERATURES IN THE ENGINE INLET REGION.

7

HEAT FLUX
3405 kW/m²

DEGREE,
°C

CONTACT CONDUCTANCE
1420 W/m²-K

WALL
TEMPERATURE,
649 °C

1112
1035
958
881
803
726
649
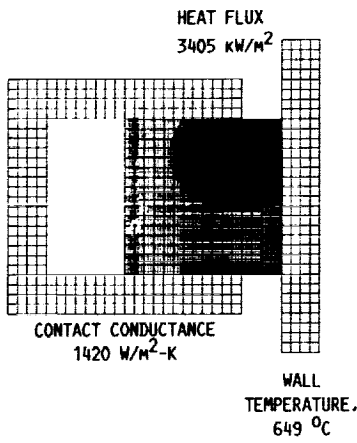
FIGURE 9. - CERAMIC WAFER SEAL TEMPERATURE DISTRIBUTION IN THE ENGINE INLET REGION.
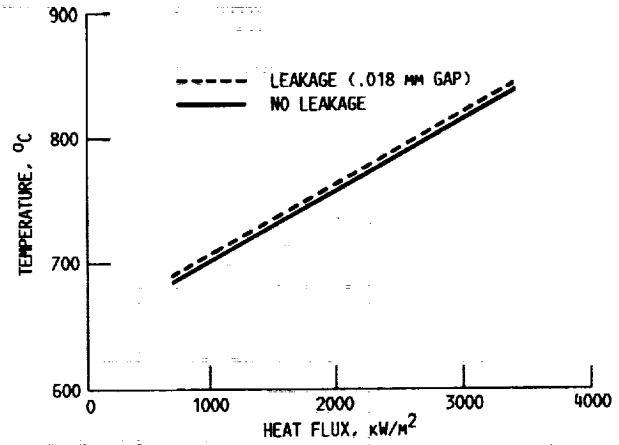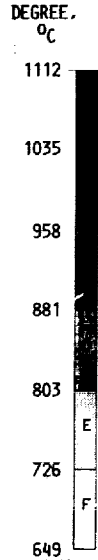
FIGURE 10. - MAXIMUM SEAL TEMPERATURES IN THE ENGINE INLET REGION WITH LEAKAGE.
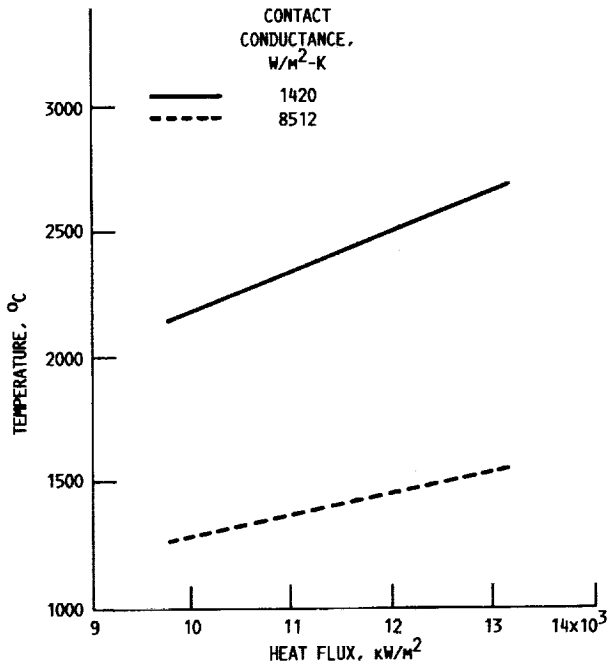
FIGURE 11. - MAXIMUM SEAL TEMPERATURES IN THE COMBUSTOR ENTRANCE REGION.

	SEAL WIDTH, MM	RECESS GAP WIDTH, MM	CONDUCTANCE, W/m²-K
○	13	3	1420
◇	13	3	8512
△	13	5	1420
▽	13	5	8512
◠	25	3	1420
▢	25	3	8512
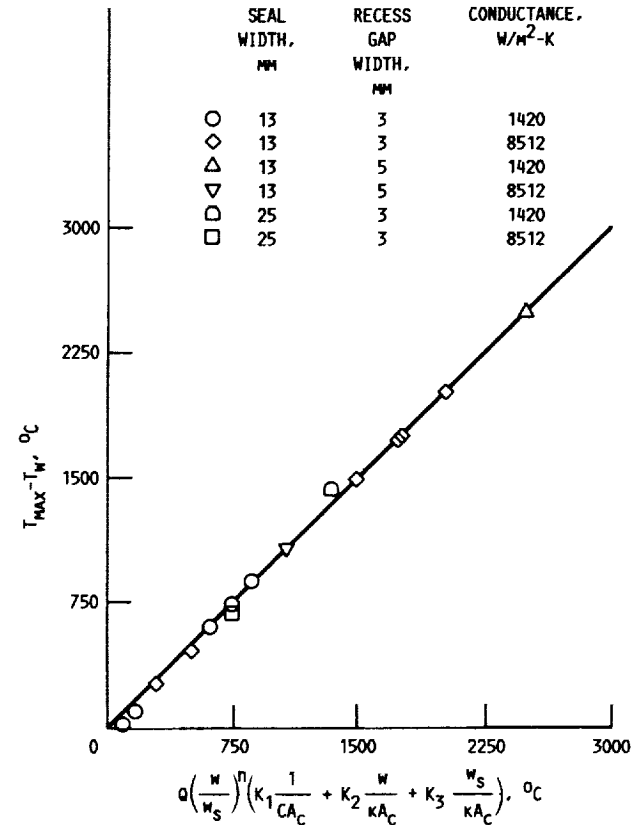
$$Q\left(\frac{W}{W_s}\right)^n\left(K_1\frac{1}{CA_c} + K_2\frac{W}{kA_c} + K_3\frac{W_s}{kA_c}\right), \ °C$$

FIGURE 12. - COMPARISON OF MAXIMUM SEAL TEMPERATURE PREDICTIONS.

8
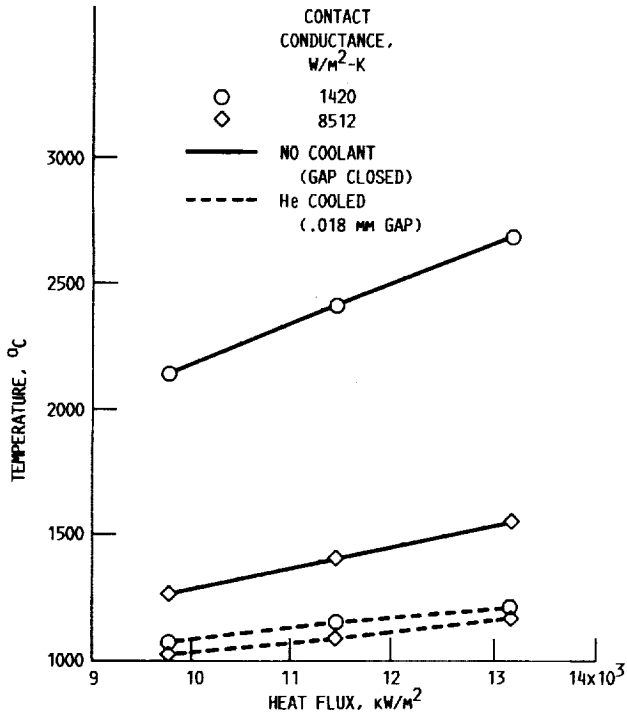
FIGURE 13. - MAXIMUM SEAL TEMPERATURES IN THE COMBUSTOR
ENTRANCE REGION WITH HELIUM COOLING.

CONTACT
CONDUCTANCE,
W/M^2-K

○   1420
◇   8512

──── NO COOLANT
(GAP CLOSED)
- - - - He COOLED
(.018 MM GAP)
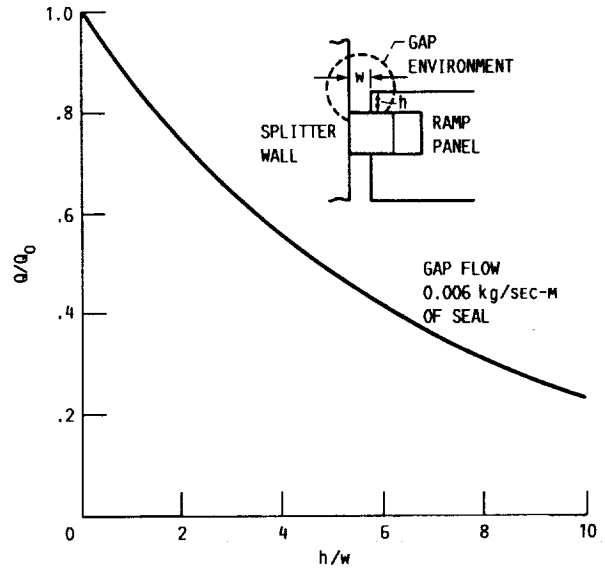
FIGURE 15. - EFFECT OF SEAL RECESS GAP DEPTH ON THERMAL
LOAD TO THE SEAL IN THE COMBUSTOR ENTRANCE REGION.

GAP FLOW
0.006 kg/SEC-M
OF SEAL
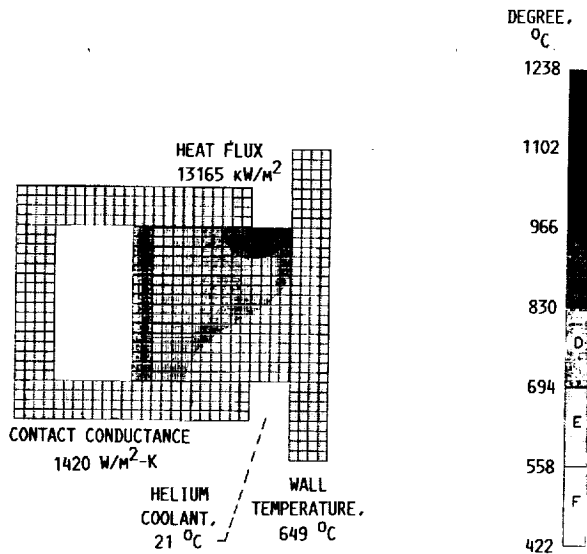
FIGURE 14. - SEAL TEMPERATURE DISTRIBUTION IN THE COMBUSTOR
ENTRANCE REGION WITH HELIUM COOLING.
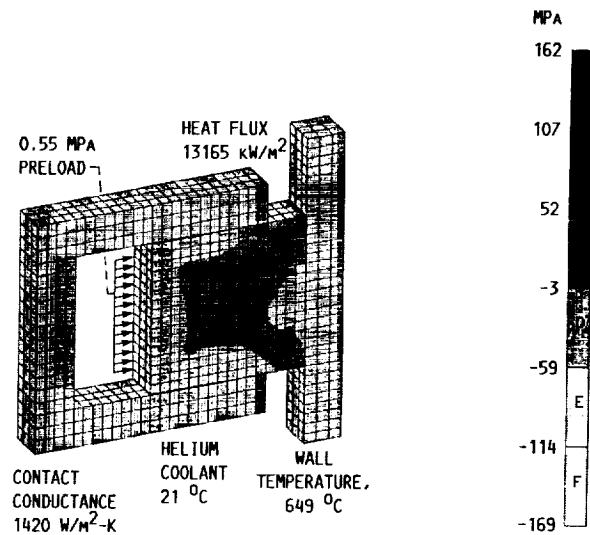
FIGURE 16. - MAXIMUM PRINCIPAL STRESS DISTRIBUTION IN THE
COMBUSTOR ENTRANCE REGION WITH HELIUM COOLING.

16. Abstract   *are numerically assessed.*

This paper numerically assesses the thermal and structural performances of a ceramic wafer seal in a simulated hypersonic engine environment. The effects of aerodynamic heating, surface contact conductance between the seal and its adjacent surfaces, flow of purge coolant gases, and leakage of hot engine flow path gases on the seal temperature were investigated from the engine inlet back to the entrance region of the combustion chamber. Finite element structural analyses, coupled with Weibull failure analyses, were performed to determine the structural reliability of the wafer seal.